Production of fiberboard from rice straw thermomechanical extrudates by thermopressing : influence of fiber morphology, water and lignin content

Dyna Theng, Gerard Arbat, Marc Delgado-Aguilar, Bunthan Ngo, Laurent Labonne, Pere Mutjé, Philippe Evon

Production of fiberboard from rice straw thermomechanical extrudates by thermopressing: influence of fiber morphology, water and lignin content

Dyna Theng[1,3] · Gerard Arbat[2] · Marc Delgado-Aguilar[1] · Bunthan Ngo[3] · Laurent Labonne[4] · Pere Mutjé[1] · Philippe Evon[4]

Abstract

The objective of this study was to investigate the influence of fiber morphology and molding parameters on the mechanical and physical properties of fiberboards made from rice straw. The rice straw was thermomechanically treated with a twin-screw extruder. Three parameters were investigated: the amount of water added at molding (0–20%), lignin content (0–25%), and the liquid/solid ratio used for extrudate production (0.33–1.07). A Doehlert experimental design was used to evaluate the effects of these factors on fiberboard properties. A liquid/solid ratio of 0.4 at extrudate production, the addition of 5% water at molding, and a lignin content of 8.9% were found to be optimal for bending properties. The fiberboard produced in these conditions had a density of 1414 kg/m^3 (i.e. the densest board). Maximum flexural strength and elastic modulus were 50.3 MPa and 8.6 GPa, respectively. A thickness swelling of 23.6% and 17.6% water absorption were observed. The statisti-cal analysis suggested that a good compromise between density and flexural properties could be obtained with the addition of 0% water, a lignin content of 25% and a liquid/solid ratio of 0.33 at extrudate production. Polynomial models suggested that the fiberboards produced in such conditions would have a maximum flexural strength of 50 MPa, an elastic modulus of 6.0 GPa, a density of 1102 kg/m^3, and a thickness swelling of 24%.

1 Introduction

Lignocellulosic biomass has recognized potential for use in the production of natural composites. The use of biomass for such applications generally requires mechanical, thermal or chemical pretreatment, or a combination of these methods (Zhang et al. 2015). Like all lignocellulosic materials, rice straw consists principally of cellulose and hemicelluloses. These two carbohydrate polymers form a heterogeneous complex. Hemicelluloses are impregnated with layers of lignin, which form a three-dimensional hydrophobic network around cellulose/hemicellulose complexes. Lignin provides plants with rigidity and renders them impermeable to water and highly resistant to decomposition. The release of cellulose and hemicelluloses therefore requires pretreatment to break down the lignin that protects them. As an example, the defibration of different lignocellulosic biomass sources was recently conducted through twin-screw extrusion using thermo-mechanical and thermo-mechano-chemical pretreatments. The wall polymers were thus destructured. And, once released, cellulose was in that specific case subsequently transformed into glucose through enzymatic hydrolysis (i.e. saccharification) and then into second-generation bioethanol (Vandenbossche et al. 2016).

Extrusion is a promising thermomechanical pretreatment for use in biomass conversion because it is cheap, the monitoring of temperature and screw speed is good, and it has

✉ Philippe Evon
Philippe.Evon@ensiacet.fr

[1] LEPAMAP Research Group, University of Girona, C/Maria Aurèlia Capmany, 61, 17003 Girona, Spain

[2] Department of Chemical and Agricultural Engineering and Food Technology, University of Girona, C/Maria Aurèlia Capmany, 61, 17003 Girona, Spain

[3] Royal University of Agriculture, Phnom Penh 2696, Cambodia

[4] Laboratoire de Chimie Agro-industrielle (LCA), Université de Toulouse, ENSIACET, INRA, INPT, Toulouse Cedex 4, France

high shear and excellent processing capacities. Single-screw and twin-screw extruders are widely used in the snack food, feed, plastic, and composites industries. However, although both types of extruders are used, twin-screw extruders are preferable to single-screw extruders, because they provide greater control over residence time distribution and mixing and have a higher capacity for heat and mass transfer (Lin et al. 2012).

Twin-screw extrusion technology has been proposed as a powerful original solution for the biorefining of whole sunflower plants (Evon et al. 2010). The twin-screw extruder results in highly effective, mechanical cell lysis in a single step, as part of a continuous process (Evon et al. 2015). Vandenbossche et al. (2015) recently used twin-screw extrusion technology for the thermomechanical and thermomechanochemical pretreatment of different lignocellulosic biomass sources for the biocatalytic production of second-generation bioethanol rather than for the manufacture of composite materials. Twin-screw extruder use for the pretreatment of fibers from agricultural waste for composite production (e.g. fiberboard manufacturing) is cheaper than the other fiber-removing technologies. For example, it is cheaper than digestion plus defibration with a rotary digester and a Sprout-Waldron defibrator by a factor of about nine (Theng et al. 2017a). Moreover, as no compound is removed from the solid material during thermomechanical treatment in the twin-screw extruder, the chemical and thermal properties of the extrudate obtained are similar to those of the raw biomass (i.e. rice straw).

As the extrudate is a mixture of lignocellulosic fibers, it could potentially be processed by thermopressing into cohesive fiberboards. Evon et al. (2014, 2015) recently described the production of self-bonded fiberboards from a cake generated during the biorefining of whole sunflower plants in a Clextral (France) BC 45 twin-screw extruder, with a heated hydraulic press. Furthermore, the proteins in the cake acted as a natural binder within the boards, ensuring their mechanical cohesion.

For rice straw extrudates, fiberboard cohesion could be achieved by adding lignin. Indeed, lignin is the principal chemical used for self-bonding and water resistance in the production of molded fiber-based objects without binding agents (Mason 1928). The lignin is melted, and a welding effect is generated during the molding operation. According to Van Dam et al. (2004), steam explosion lignin and organosolv lignin are highly reactive and can be used as a bonding agent for particle boards. They could replace up to 50% of synthetic binders (i.e. phenol-based resins), although it remains unclear how effective they would be for such an application at an industrial scale (Gosselink et al. 2011). Kraft and organosolv lignins have recently been successfully used for the production, at laboratory scale, of fiberboards from corn stalk (Theng 2017) and wheat straw (Domínguez-Robles et al. 2017) thermomechanical pulps, and from raw shives (Evon et al. 2018), a by-product of the continuous mechanical extraction of fibers from linseed straw (Ouagne et al. 2017). Indeed, the addition of 15% or 25% Kraft lignin to the thermomechanical pulp (wt% relative to wheat straw and corn stalks, respectively) increased the maximum flexural strength from 52.8 to 96.8 MPa and from 29.6 to 69.1 MPa, respectively. Similarly, the addition of 25% organosolv lignin to raw shives (wt%) also resulted in a large increase in maximum flexural strength (from 2.1 to 8.0 MPa), highlighting the potential of this form of lignin to act as a natural binder in fibrous materials. Nevertheless, despite the addition of organosolv lignin, the final flexural properties of the fiberboard remained limiting for subsequent uses.

This study assessed the feasibility of producing novel biodegradable fiberboards by the thermopressing of rice straw extrudates prepared with a Clextral Evolum HT 53 pilot-scale twin-screw extruder. It also investigated the effects of the molding parameters (i.e. the amount of water added during molding, lignin content, and the liquid/solid ratio used for extrudate production) on the mechanical and physical properties of the fiberboard.

2 Materials and methods

2.1 Materials

The starting material was a single batch of rice straw (*Oriza sativa* L.), corresponding to whole plants excluding the panicle and the grain. The rice straw was of French origin and it was purchased from JCL AGRI (Bouge-Chambalud, France). The rice was harvested in October, when the plants were mature. The rice straw had a moisture content of $7.4 \pm 0.2\%$ (French standard NF V 03-903). Its chemical composition, expressed as a percentage of dry matter, was $14.7 \pm 0.1\%$ minerals (French standard NF V 03-322), $37.7 \pm 0.3\%$ cellulose (ADF-NDF method), $27.9 \pm 0.4\%$ hemicelluloses (ADF-NDF method), $7.2 \pm 0.1\%$ lignin (ADF-NDF method), and $16.0 \pm 0.1\%$ water-soluble components (mass loss after 1 h in boiling water). The straw was crushed with a hammer mill (Elecra BC P, France) fitted with a 6 mm screen before extrudate production.

The lignin powder used in this study was supplied by CIMV (Compagnie Industrielle de la Matière Végétale, Labège, France). This product, Biolignin™, was a brown powder obtained from wheat straw (CIMV TBC 2014). The main characteristics of Biolignin™ are presented in Table 1.

The rice straw was subjected to thermomechanical fractionation with a pilot-scale Clextral (France) Evolum HT 53 copenetrating and corotating twin-screw extruder, which was used to produce the materials (i.e. the extrudates) used

Table 1 Chemical composition, molecular weight and granulometry of the CIMV Biolignin™ extracted from wheat straw

	Water (%)	Chemical composition (% of dry matter)				Molecular weight (mmol/g)			Granulometry	
		Klasson lignin (AIL + ASL)	Hemicelluloses	Ash	Proteins	Aromatic –OH	Aliphatic –OH	–COOH	< 232 µm	< 900 µm
Biolignin™	< 4	89	≤ 4	1.1	≈ 7	2.0 ± 0.2	2.1 ± 0.1	0.6 ± 0.0	90%	10%

for fiberboard manufacture. Extrudates were obtained with three different liquid/solid (L/S) ratios at extrusion: 1.0, 0.7 and 0.4. Extrudate preparation (including the extrusion process, the sampling procedure, and the description of the equipment used for defibring) is described in detail in Supplementary Material 1. The extrudates were crushed with a hammer mill (Electra VS 1, France) fitted with a 15 mm screen before molding to minimize the risk of defects such as aggregation, degassing, and blisters within the fiberboard after thermopressing. The extrudates had a moisture content of about 7% (French standard NF V 03-903). The dry weight of extrudate used for each molding experiment was 100 g (i.e. 444 mg/cm^2).

2.2 Fiber matrix preparation before molding

Biolignin™ (Table 2) and 500 mL distilled water were mixed in the desired proportions with 100 g dry weight of extruded fibers. More water than required to achieve the moisture content at molding was added at this point to guarantee the efficient mixing of lignin powder and extruded fibers. The mixture was then thoroughly stirred manually in a plastic container and allowed to dry on a nylon cloth in the air overnight at room temperature. The prepared material was dried in a ventilated oven at 80 °C during the morning of the following day until the desired moisture content for molding was reached. Depending on the thermopressing conditions used, the achievement of this moisture content required the addition of 0.0 to 20.0% water at molding (percentage in weight, expressed as a proportion of the dry weight of the extruded fibers) (Table 2).

2.3 Thermopressing

Molding was performed by thermopressing in an aluminum mold. A 400-metric ton capacity Pinette Emidecau Industries (France) heated hydraulic press was used to produce 3 mm × 150 mm × 150 mm fiberboards. Fourteen fiberboards were manufactured with different molding parameters in a Doehlert experimental design with three variables: amount of water added at molding (from 0 to 20% in weight, as a proportion of the dry weight of the extruded fibers), lignin content (from 0 to 25% in weight, as a proportion of the dry weight of the extruded fibers) and the liquid/solid (L/S) ratio used for extrudate production (from 0.33 to 1.07) (Table 2).

The minimum values for the amount of water added at molding and lignin content were set to 0%, to simulate the direct hot pressing of rice straw extrudates, corresponding to no addition of water or ligneous binder at molding. The maximum values (20% and 25%, respectively) were set so as to be of the same order of magnitude as in a previous study by Theng et al. (2017b), in which a corn-stalk thermomechanical pulp was used as the raw material and kraft lignin as a green adhesive. For the L/S ratio at extrusion, the minimum and maximum values used were those used by Theng et al. (2017a) in a previous study, in which rice straw was used as the starting material. With an L/S ratio below 0.33, fiber length would have been greatly reduced during the twin-screw defibration treatment, and total production costs would have been much higher. By contrast, the use of L/S ratios exceeding 1.07 would have resulted in the filling of the twin-screw machine with water right back to the feed module, preventing the correct introduction of the rice straw.

The Doehlert experimental design used here is presented in Table 2. This table refers to the three coding values (X_i, with i ranging from 1 to 3) tested for the manufacture of each of the 14 fiberboards, related to the three molding parameters studied: amount of water added at molding, lignin content and L/S ratio during extrusion, respectively. Experimentally, the real molding parameters used for the production of fiberboards 1 to 14 were calculated from these coding values, each of which could vary between − 1.0 (associated with the minimum value of the corresponding molding parameter) and 1.0 (associated with the maximum value of the corresponding molding parameter). These molding parameters also appear in Table 2.

The other molding conditions (i.e. the pressure applied, mold temperature and molding time) were fixed as non-variable parameters, with two cycles of pressing, as follows:

1. Hot pressing at 22.3 MPa (pressure expressed as the force per unit area of molded fiberboard) and 200 °C for 5 min. Pressure was then decreased, at a rate of 0.2 MPa/s, to 1.0 MPa, with temperature held constant. The temperature was then decreased to 60 °C while maintaining an applied pressure of 1.0 MPa. The mold was then opened under automatic control. Including the

Table 2 Molding parameters for the manufacture of the 14 fiberboards (Doehlert experimental design)

Board number	X_1	Water added at molding (%)	X_2	Lignin content (%)	X_3	L/S ratio during extrusion
1	1.000	20.0	0.000	12.5	0.000	0.7
2	− 1.000	0.0	0.000	12.5	0.000	0.7
3	0.500	15.0	0.866	23.3	0.000	0.7
4	− 0.500	5.0	− 0.866	1.7	0.000	0.7
5	0.500	15.0	− 0.866	1.7	0.000	0.7
6	− 0.500	5.0	0.866	23.3	0.000	0.7
7	0.500	15.0	0.289	16.1	0.816	1.0
8	− 0.500	5.0	− 0.289	8.9	− 0.816	0.4
9	0.500	15.0	− 0.289	8.9	− 0.816	0.4
10	0.000	10.0	0.577	19.7	− 0.816	0.4
11	− 0.500	5.0	0.289	16.1	0.816	1.0
12	0.000	10.0	− 0.577	5.3	0.816	1.0
13	0.000	10.0	0.000	12.5	0.000	0.7
14	0.000	10.0	0.000	12.5	0.000	0.7

cooling step, this first cycle lasted about 30 min in total. Each panel was then cooled at room temperature for 2.5 h, and no significant change in its moisture content was observed during this cooling step.

2. After cooling, the fiberboard was hot-pressed again at 11.2 MPa and 200 °C for 1 min. The same procedure as for the first cycle was then followed, with a decrease in pressure to 1.0 MPa, followed by a decrease in temperature to 60 °C before the automatic opening of the mold. Including the cooling step, this second cycle lasted about 20 min in total.

The molding temperature used here (200 °C) is higher than the lignin glass transition temperature. This temperature was used to ensure that the Biolignin™ remained in a rubbery state during molding. It was selected based on an earlier study (Mancera et al. 2012) for which, to be accurate, a 205 °C molding temperature was used. Given the TGA results for Biolignin™ and rice straw thermomechanical extrudates (Theng et al. 2017a), this molding temperature was also below the lowest temperature at which the thermal degradation of organic compounds occurs in both the binder and the lignocellulosic fibers of extrudates. The pressure applied and the molding duration were chosen as appropriate for the target fiberboard thickness of 3 mm, according to the results of previous studies (Anglès et al. 2001; Mancera et al. 2012; Theng et al. 2017b).

Statistical analysis was conducted with NEMRODW® software (NEMRODW 2015), which was also used to plot the isoresponse curves.

The best-fit second-order response (Y) obtained for each characteristic of the fiberboard (i.e. flexural properties, Charpy impact strength, Shore *D* surface hardness, thickness swelling, water absorption, and color) is given by the following formula:

$$\begin{aligned} Y = {} & a_0 + (a_1 \times X_1) + (a_2 \times X_2) + (a_3 \times X_3) \\ & + (a_{11} \times X_1 \times X_1) + (a_{22} \times X_2 \times X_2) \\ & + (a_{33} \times X_3 \times X_3) + (a_{12} \times X_1 \times X_2) \\ & + (a_{13} \times X_1 \times X_3) + (a_{23} \times X_2 \times X_3) \end{aligned} \quad (1)$$

where X_1, X_2, and X_3 are the coding values of the experimental design, each varying from − 1.0 to 1.0, and relating to the three molding parameters tested (amount of water added at molding, lignin content, and L/S ratio used for extrudate production, respectively), and a_i (*i* varying from 0 to 3), and a_{ij} (*i* and *j* varying from 1 to 3, and $i \leq j$) are the coefficients of the polynomial model.

For each fiberboard characteristic, the significance of the coefficients of the best-fit second-order response was estimated by comparing absolute values with the associated standard deviations. The a_i and a_{ij} coefficients were considered significant when their absolute values were higher than the standard deviation, and non-significant if their absolute values were lower than the standard deviation.

Three fiberboards were produced for each of the molding conditions tested, to assess reproducibility. Immediately after molding, these fiberboards were transferred to a climatic chamber (60% RH, 25 °C), in which they were stored for 4 weeks for conditioning. The first fiberboard was used for the assessment of thickness, apparent density, and mechanical properties relating to bending. After conditioning, four 30 mm-wide test specimens were cut. The thickness of these specimens was measured at three points and their length was measured at two points, to within 0.01 mm, with an electronic digital sliding caliper. Thickness, length and

weight were recorded for the calculation of specimen volume and density. The thickness (t) and apparent density (d) of the fiberboard were calculated as the means of the measurements taken on the four test specimens. A second fiberboard was used to measure Shore D surface hardness and Charpy impact strength. The third fiberboard was used for the evaluation of thickness swelling and water absorption.

2.4 Mechanical properties for bending

The flexural properties of the test specimens were assessed according to French standard NF EN 310, with an Instron 33R4204 (USA) universal testing machine fitted with a 500 N load cell, and the three-point bending technique. The test specimens were 150 mm long and 30 mm wide. Their thickness was measured to within 0.01 mm with an electronic digital sliding caliper. The testing speed was 2 mm/min, with a grip separation of 100 mm. The load was applied equidistant from the two supports, and the loading direction was perpendicular to the upper surface of the test specimen. The properties evaluated included breaking load (F), maximum flexural strength (σ_f), and elastic modulus (E_f). All determinations were carried out four times, once on each of the four test specimens cut from each fiberboard.

2.5 Charpy impact strength

The impact strength of unnotched test specimens was assessed according to French standard NF EN ISO 179 with a Test-well Wolpert 0–40 daN cm (France) Charpy machine, which was also used to measure absorbed energy (W), and impact resilience (K). Eight test specimens, each 60 mm long and 10 mm wide, were cut. Section thickness was measured at three points, to within 0.01 mm, with an electronic digital sliding caliper, and the mean value was determined. Impact strength was measured at 23 °C by the three-point bending technique with a grip separation of 25 mm. The load was applied equidistant from the two supports, and the loading direction was perpendicular to the test specimen. All determinations were carried out eight times, once on each of the eight test specimens cut from each fiberboard.

2.6 Shore D surface hardness

The Shore D surface hardness of the fiberboards was assessed with a Bareiss (Germany) durometer according to French standard NF EN ISO 868. The direction of indentation was perpendicular to the upper surface of the fiberboard. All determinations were carried out 48 times for each fiberboard (24 times for each side of the board).

2.7 Color measurement

The color of the fiberboard specimens was determined with a Konica Minolta CR-410 (Japan) spectrophotometer. Color was assessed with the CIE L*a*b* reference, which is widely used for non-luminous objects. The illuminant was D65, and the observer angle was 2°. In the L*a*b* color space, L* is the lightness, and it varies from 0 (black) to 100 (white), and a* and b* are the chromaticity coordinates: + a* is the red direction, − a* is the green direction, + b* is the yellow direction, and − b* is the blue direction. The center is achromatic (Konica Minolta Sensing 2007). All determinations were carried out 48 times on each fiberboard specimen (24 times for each side of the board).

The measured L* color values were used to estimate the darkening of the fiberboard relative to the starting material, rice straw. The difference in color (ΔE*) between the rice straw and each fiberboard was calculated as follows:

$$\Delta E* = \sqrt{(\Delta L*)^2 + (\Delta a*)^2 + (\Delta b*)^2} \quad (2)$$

2.8 Thickness swelling and water absorption

Four 50 mm × 50 mm samples were used to determine the thickness swelling (TS) and water absorption (WA) of the fiberboards. The fiberboards were submerged in distilled water at 25 °C for 24 h. TS was calculated according to French standard NF EN 317, and the thickness of each sample was measured at four points midway along each side, 10 mm from the edge, before and after soaking in distilled water. Each sample was also weighed to an accuracy of 0.01 g to estimate WA values, where

$$WA = (m_2 - m_1)/m_1 \times 100 \quad (3)$$

and m_1 and m_2 are the masses of the sample before and after immersion.

2.9 Analytical methods

Prior to each analysis, the materials (i.e. rice straw and extrudates) were milled with a Foss (Denmark) Cyclotec 1093 cutting mill fitted with a 1 mm screen. Moisture content was determined according to the French standard NF V 03-903. Mineral content was determined according to French standard NF V 03-322. The amounts of the three cell wall constituents (cellulose, hemicelluloses, and lignins) were estimated by the ADF-NDF method of Van Soest and Wine (1967, 1968). The water-soluble component content was assessed by measuring the mass loss of the test sample after 1 h in boiling water. All analyses were carried out in duplicate.

2.10 Thermogravimetric analysis

Thermogravimetric analysis (TGA) was performed on Biolignin™ with a Shimadzu TGA-50 (Japan) analyzer. Dynamic analysis was conducted in air, with the temperature increasing from 25 to 800 °C, at a rate of 5 °C/min. The mass of the test sample was about 8 mg. Sample mass was determined at various temperatures. These data were later used to plot the percentage of undegraded sample (1 - D) (%) as a function of temperature, where

$$D = (W_0 - W)/W_0 \quad (4)$$

and W_0 and W are the weights at the starting point and during scanning (mg). Measurements were carried out in duplicate.

2.11 Morphological analysis of fibers in extrudates

A MorFi Compact analyzer (TechPap, France) equipped with a CCD video camera was used for the morphological analysis of extrudates. About 30,000 fibers were analyzed with MorFi v9.2 software. This software calculated a number of parameters, including mean fiber length, mean diameter and the fines percentage (fibers shorter than 76 µm). A sample of 2.5 g of dry extrudate was diluted in 1000 mL distilled water, with mechanical stirring to break up aggregates. A 100 mL aliquot of the mixture was taken and diluted (1:10) by adding distilled water to make the volume up to 1000 mL. This process was repeated twice until a consistent concentration of 25 mg/L was achieved. All characterizations were performed in duplicate.

2.12 Apparent and tapped densities

Tapped density was measured with a Granuloshop Densitap ETD-20 (France) volumenometer fitted with a 250 mL graduated cylinder. Apparent density was also measured before compaction. All measurements were performed in duplicate.

2.13 Statistical analysis

For both the chemical composition and fiber morphology of extrudates, all determinations were conducted in duplicate. Data are expressed as means ± standard deviations. The means were compared by one-way analysis of variance (ANOVA) with PAWS Statistics 18 software. The various individual means were compared in Duncan's multiple range test with a significance level of 5%. Thus, in the two related tables, means in the same column and with the same superscript letter were not significantly different at the 5% level.

3 Results and discussion

3.1 Physicochemical characterization of the extrudates

Table 3 shows the chemical composition of rice straw before and after twin-screw extrusion. The thermomechanical treatment applied in the twin-screw extruder had no marked effect on composition at high (1.0, i.e. E_1 extrudate) or low (0.4, i.e. E_3 extrudate) L/S ratios. Indeed, the chemical compositions obtained were similar to cellulose, hemicellulose, lignin, and water-soluble component contents of 34 to 38%, 28 to 33%, 6 to 7%, and 16 to 17%, respectively. The extrudates were also subjected to thermal gravimetric analysis (see Supplementary Material 2). As for chemical composition, TGA results were similar for rice straw and extrudates, indicating that the thermomechanical treatment applied to the rice straw did not increase its thermal stability.

The morphological analysis of the fibers in the three extrudates (E_1–E_3) was conducted with a MorFi Compact analyzer, and the micrographs obtained are shown in Fig. 1. The main morphological characteristics of these fibers, produced under different operating conditions (extrudates E_1–E_3), before and after crushing in a hammer mill fitted with a 15 mm screen, were recorded (Table 4). A MorFi Compact analyzer was used to assess these characteristics, which included the length, diameter and aspect ratio (defined as the ratio of length to diameter) of fibers, together with the fine content of the extrudates. Based on the mean length (L_W) and diameter (D) of the extruded fibers, the corresponding L_W/D aspect ratios were in the 20.9–22.6 range before crushing. The decrease in aspect ratio observed with decreases in L/S ratio from 1.0 to 0.4 resulted principally from a decrease

Table 3 Chemical composition of rice straw biomass and rice straw extrudates obtained after thermomechanical fractionation in the Clextral Evolum HT 53 twin-screw extruder (% of dry matter)

Material	Minerals	Cellulose	Hemicelluloses	Lignin	Water-soluble components
Rice straw	14.7 ± 0.1^{a}	37.7 ± 0.3^{a}	27.9 ± 0.4^{a}	7.2 ± 0.1^{a}	16.0 ± 0.1^{a}
E_1 (1.0 L/S ratio)	14.3 ± 0.2^{a}	36.2 ± 0.5^{a}	33.0 ± 0.6^{b}	5.5 ± 0.5^{b}	15.9 ± 0.1^{a}
E_2 (0.7 L/S ratio)	14.4 ± 0.1^{a}	37.0 ± 0.9^{a}	28.4 ± 0.2^{a}	6.8 ± 0.3^{a}	17.3 ± 0.3^{b}
E_3 (0.4 L/S ratio)	15.8 ± 0.0^{b}	33.8 ± 0.1^{b}	29.3 ± 0.2^{a}	$6.3 \pm 0.2^{a,b}$	16.2 ± 0.2^{a}

Means in the same column with the same superscript letter (a, b) are not significantly different at the 5% significance level

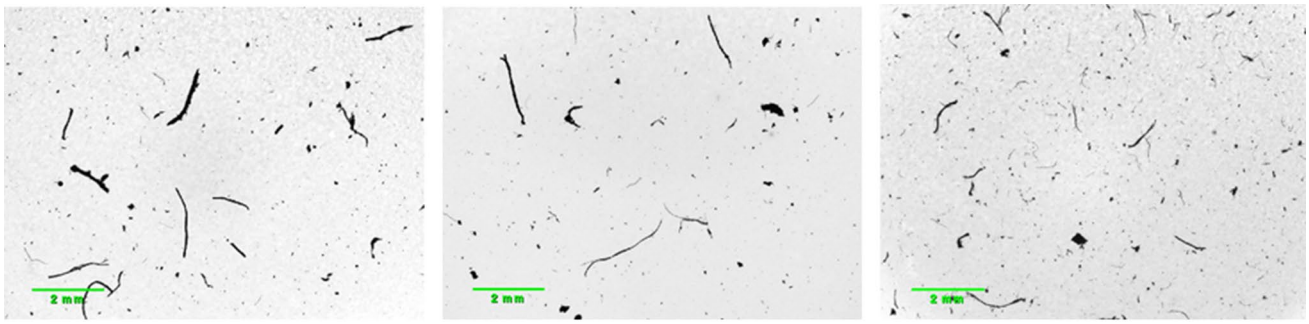

(a) (b) (c)

Fig. 1 Micrographs of fibers in extrudates **a** E1, **b** E2 and **c** E3 obtained during morphological analyses with the MorFi Compact analyzer

Table 4 Morphological properties of extrudates before and after crushing in an Electra VS 1 hammer mill fitted with a 15 mm screen

Material	L_W (µm)	D (µm)	L_W/D (aspect ratio)	Fines (%)
Before crushing				
E_1 (1.0 L/S ratio)	571.5 ± 7.8^a	25.5 ± 0.0^a	22.4 ± 0.3^a	63.8 ± 0.4^b
E_2 (0.7 L/S ratio)	571.0 ± 7.1^a	25.3 ± 0.0^a	22.6 ± 0.3^a	54.2 ± 4.9^a
E_3 (0.4 L/S ratio)	494.0 ± 1.4^b	23.7 ± 0.1^b	20.9 ± 0.1^b	61.9 ± 0.5^b
After crushing				
E_1 (1.0 L/S ratio)	346.0 ± 7.1^a	23.1 ± 0.1^a	15.0 ± 0.4^a	86.6 ± 0.7^a
E_2 (0.7 L/S ratio)	306.0 ± 8.5^b	23.4 ± 0.6^a	13.1 ± 0.0^b	75.1 ± 1.3^b
E_3 (0.4 L/S ratio)	270.0 ± 2.8^c	23.8 ± 0.4^a	11.3 ± 0.3^c	66.7 ± 3.5^c

Means in the same column with the same superscript letter (a, b before crushing and a–c after crushing) are not significantly different at the 5% level

in the mean length of fibers from 571 to 494 µm (i.e. − 14%) (Table 4). Thus, the higher mechanical shear and greater self-heating of the material generated at the level of the reversed screws when low L/S ratios were used in the twin-screw extruder resulted in more intense fiber cutting. The morphological properties of the fibers in extrudates E_1 and E_2 (i.e. 1.0 and 0.7 L/S ratios, respectively) were clearly not significantly different. By contrast, the fibers in extrudate E_3 (i.e. 0.4 L/S ratio) were significantly shorter.

Table 4 also shows the morphological properties of extrudates after their passage through a hammer mill fitted with a 15 mm screen. Depending on the L/S ratio used for extrudate production, the mean length and mean aspect ratio of fibers were in the 346–270 µm and 15.0–11.3 ranges, respectively. The decrease in mean length indicates that the hammer mill not only broke up fiber aggregates but also cut the fibers. The aspect ratio after passage through the hammer mill was about 50% lower than that in the extruded fibers before crushing. After the crushing step, the shortest fibers and the lowest aspect ratio were obtained with the lowest value of L/S ratio used for extrudate production (i.e. 0.4). The mean length and mean aspect ratio of the fibers of the three extrudates were significantly different.

Longer fibers generally make for greater strength in composite materials. However, Shen (1986) claimed that the smaller size of the fibers in composite products made from sugar (used here as a bonding agent) and different lignocellulosic materials (e.g. sugarcane bagasse, and stalks of sorghum, corn, sunflower, flax) might also have a positive effect during molding, by increasing the specific surface area and the accessibility to inner cell wall components, thereby improving the mechanical properties of the fiberboard. The crushing step was performed principally to break up fiber aggregates, thereby facilitating mixing of the extrudate, lignin and water, but it also helped to shorten the fibers (Table 4). It is, therefore, reasonable to assume that this cutting might improve the bending properties of the boards.

An analysis of the distribution of the morphological subgroups of fibers in the extrudates (Table 4) also revealed the presence of small particles (fibers shorter than 76 µm). This population contained not only the shortest fibers but also spherical particles of small diameter originating from the thermomechanical breakdown of rice straw together with the additional crushing step, corresponding to 63.8% and 86.6% of the maximal values before and after crushing, respectively. Finally, the

apparent and tapped densities of the extrudates were low, with maximal values before crushing of 162 kg/m^3 and 216 kg/m^3, respectively, and maximal values after crushing of 104 kg/m^3 and 145 kg/m^3, respectively (Fig. 2).

3.2 Thermal stability of Biolignin™

Lignin powder was added to the rice straw extrudates at levels of 0 to 25%, values similar to those used in previous studies (Anglès et al. 2001; Mancera et al. 2012; Theng et al. 2017b). According to Mason (1928) and Back (1987), lignin, thanks to its polyphenolic structure, is the most important chemical for self-bonding (i.e. intra-fiber bonding) and for water resistance in fiber-based objects molded without synthetic resin. During molding by thermal pressing, the matrix components, including lignin, flow out of the cell walls to fill the gaps between fiber particles (Takahashi et al. 2010). The presence of water facilitates the separation of cell wall components during flow testing at high pressure (Yamashita et al. 2009), due to the lower softening point of lignin (plasticization) and better heat transfer (Xu et al. 2006). Degradation with increasing temperature has been reported during thermal pressing (Okuda et al. 2006). TGA was therefore performed on the lignin powder used in this study, and the TGA degradation curve is shown in Fig. 3. A first mass loss was observed at 100 °C, corresponding to the evaporation of water. The moisture content was about 4% (Table 1), and the percentage mass loss observed on the corresponding TGA curve was consistent with a loss of water. The thermal degradation of organic compounds occurred in two successive stages (between 150 and 325 °C, and between 350 and 450 °C), resulting in the loss of about 40% and 55%, respectively, of the test sample dry mass.

Previous studies based on thermogravimetric and differential scanning calorimetry methods have shown that a first endothermic event occurs at about 150 °C for lignin, this event being attributed to lignin fusion (Murugan et al. 2008). Other endothermic peaks were also observed at temperatures above 180 °C, and these peaks were attributed to physical and/or chemical changes in lignin. However, the complexity of lignin structure made it difficult to fully explain these changes. The irreversible change in lignin observed at temperatures above 180 °C may be related to the "lignin activation" phenomenon, in which lignin is partially depolymerized to create new linkage capability (Mobarak et al. 1982). Activated lignin would have a lower melting point and a greater capacity for polycondensation.

The second and largest TGA degradation phenomenon was observed at high temperature (i.e. 350–450 °C) and may correspond essentially to the degradation of lignin. However, as TGA was conducted in air, this second thermal degradation event may be partly due to the oxidation of the primary degradation products generated by the first degradation event (Uitterhaegen et al. 2016). In the case of Biolignin™, this would reflect the degradation of the protein and hemicellulose fractions. At the end of TGA measurement, the undegraded sample accounted for less than 2% of the test sample mass, corresponding to the minerals present in the lignin powder (Table 1). In conclusion, given that the molding temperature was 200 °C and the thermal degradation of lignin occurred at temperatures at or above 350 °C, it is reasonable to assume that the ligneous binder did not undergo thermal degradation during molding.

3.3 Mechanical and physical properties of fiberboards

All the fiberboards generated were cohesive (see Supplementary Material 3), including those to which minimal amounts of lignin were added (i.e. only 1.7%). They all had densities in the 1239–1414 kg/m^3 range (Table 5), and these renewable materials could therefore be considered hardboards. The density of the equilibrated fiberboards was not significantly affected by all the molding parameters tested.

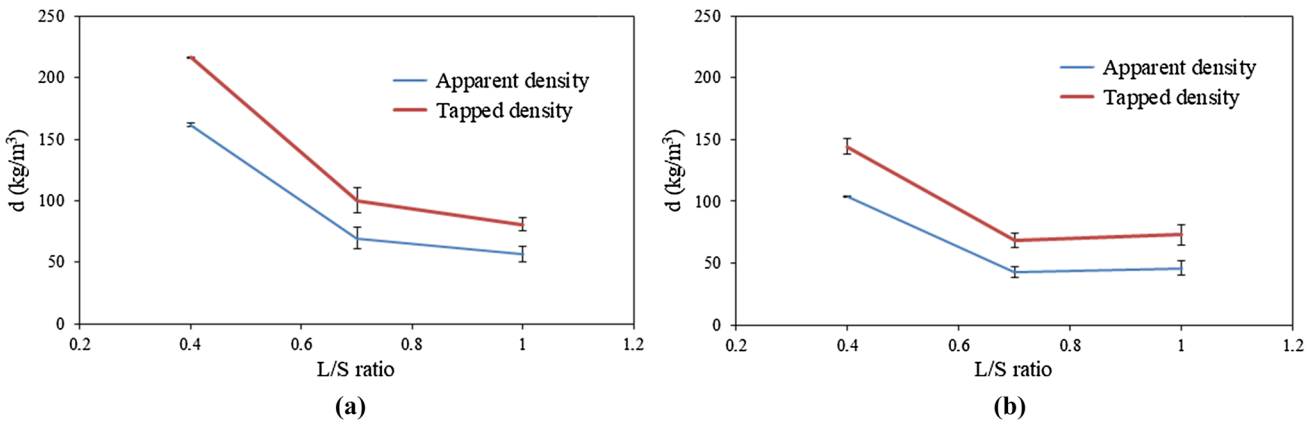

Fig. 2 Apparent and tapped densities of extrudates **a** before and **b** after crushing

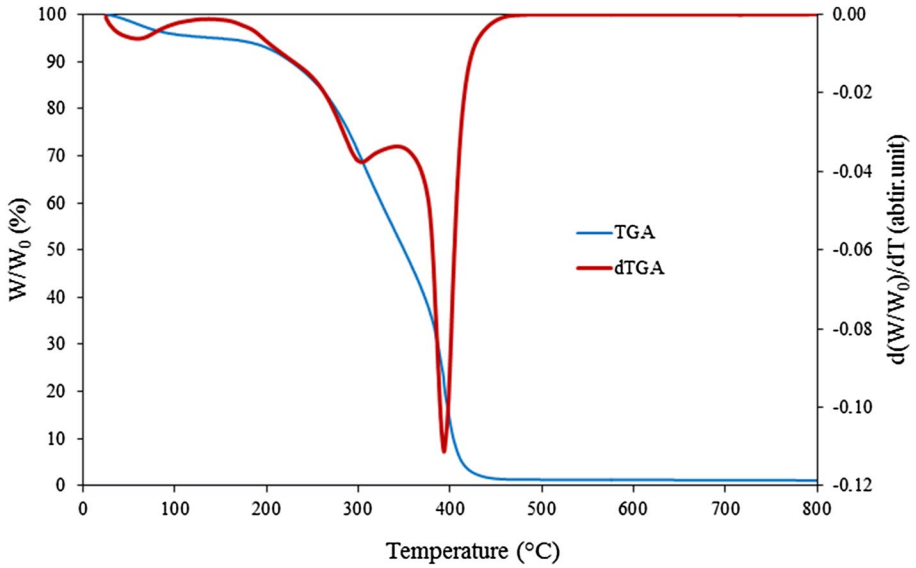

Fig. 3 TGA and dTGA curves of Biolignin™ extracted from wheat straw (from CIMV)

This was demonstrated by the very low value for the a_3 coefficient of the associated polynomial model (i.e. 4.5), relative to the values of a_1 and a_2 (i.e. −23.9 and −41.5, respectively) (Table 6). Furthermore, as the a_1 and a_2 coefficients were negative, the addition of larger amounts of water during molding and/or especially of larger amounts of lignin would lower the density of the fiberboard. By contrast, although non-significant, the a_3 coefficient was positive, indicating that an increase in the L/S ratio used for extrudate production would tend to make the fiberboard slightly denser. The densest board generated in this study was panel 8 (1414 kg/m^3), which was generated with values below the center of the experimental domain for both the amount of water added at molding and lignin content (5% and 8.9%, respectively). The L/S ratio used during extrusion for this board was 0.4. Conversely, the two boards with the lowest densities, boards 6 and 10 (1239 kg/m^3 and 1242 kg/m^3, respectively), were both generated in conditions in which large amounts of lignin were added (23.3% and 19.7%, respectively).

All the correlation coefficients obtained for the various polynomial models exceeded 0.82, with the exception of those relating to bending properties, for which the correlation coefficient ranged from 0.52 to 0.58. Thus, the best-fit second-order responses for maximum flexural strength and elastic modulus were further from the values obtained experimentally than those for the other fiberboard characteristics analyzed. However, according to the polynomial models relating to breaking load, maximum flexural strength and elastic modulus, bending properties improved with increasing lignin content within the material, as illustrated by the positive values of the associated a_2 coefficients (Table 6). This finding confirmed the ability of lignin to act as a binder within boards, as demonstrated by comparisons of the flexural properties of boards 5 and 3, and then of boards 4 and 6, in which lignin content increased from 1.7 to 23.3% with no change in the amount of water (15% and 5%, respectively) or the L/S ratio (0.7) (Table 5). By contrast, the other two molding parameters (amount of water added at molding and L/S ratio during extrusion) had negative effects on the mechanical properties of fiberboards, as the a_1 and a_3 coefficients were negative (Table 6). Nevertheless, it should be noted that the a_3 coefficient was not significant for the maximum flexural strength response. Similarly, the a_2 coefficient was not significant for the elastic modulus response. Thus, the addition of larger amounts of water at molding and the use of a high L/S ratio for extrudate production results in more brittle, less bendable boards. This finding of a negative impact of moisture content on mechanical properties is consistent with the results of Miki et al. (2003) and Mobarak et al. (1982). The addition of larger amounts of water probably improves lignin mobilization during molding through plasticization (Yamashita et al. 2007, 2009). However, as the matrix is still wet at the opening of the hydraulic press, it may also result in degassing phenomena. Degassing was indeed observed for the largest amounts of water added at molding, particularly for boards 1 and 5, for which 20% and 15% water, respectively, was added at molding. It resulted in the appearance of cracks in these two boards, which were detected when the test specimens were cut. These defects are the most likely explanation for the mechanical fragility of boards 1 and 5 (Table 1). A high L/S ratio during extrusion (1.0) resulted in the maintenance of longer fiber lengths (Table 4), even after crushing. Despite the higher frequency of spherical particles, it is reasonable to assume that the longer fibers obtained at an L/S ratio of 1.0 had a smaller specific surface area, contributing to the weak mechanical properties of the corresponding boards 7, 11 and 12 (Shen 1986).

Table 5 Mechanical properties of the 14 fiberboards manufactured by thermopressing

Board number	Bending properties							Surface hardness	Charpy impact strength	
	t (mm)	d (kg/m^3)	F (N)	σ_f (MPa)	E_f (GPa)	σ_f/d (kPa.m^3/kg)	E_f/d (MPa.m^3/kg)	Shore *D* (°)	W (mJ)	K (kJ/m^2)
1	3.6 ± 0.5	1273 ± 126	82.3 ± 9.1	27.9 ± 4.4	4.2 ± 0.9	21.8 ± 2.1	3.3 ± 0.5	78.6 ± 0.0	112.5 ± 24.9	2.4 ± 0.6
2	3.6 ± 0.2	1337 ± 48	117.7 ± 8.0	38.3 ± 3.6	5.9 ± 0.7	28.6 ± 2.2	4.4 ± 0.6	79.6 ± 0.3	158.8 ± 21.0	3.3 ± 0.4
3	3.6 ± 0.1	1360 ± 46	134.8 ± 9.9	41.6 ± 2.9	6.8 ± 0.5	30.7 ± 2.2	5.0 ± 0.3	79.7 ± 0.3	96.3 ± 18.5	1.7 ± 0.6
4	3.1 ± 0.1	1390 ± 136	74.7 ± 11.1	33.1 ± 5.5	6.2 ± 0.7	23.1 ± 5.2	4.3 ± 0.8	79.2 ± 0.0	151.4 ± 21.2	3.4 ± 0.6
5	3.2 ± 0.1	1300 ± 91	52.8 ± 7.0	22.9 ± 1.7	5.4 ± 0.5	18.2 ± 2.0	4.3 ± 0.5	78.8 ± 0.3	174.3 ± 25.1	4.3 ± 0.8
6	3.7 ± 0.1	1239 ± 145	146.2 ± 4.4	47.1 ± 6.0	7.7 ± 0.9	38.8 ± 9.2	6.3 ± 1.2	79.9 ± 0.3	135.7 ± 12.7	2.9 ± 0.7
7	3.7 ± 0.2	1324 ± 103	102.5 ± 4.1	31.1 ± 1.3	4.7 ± 0.7	23.8 ± 1.3	3.6 ± 0.2	78.7 ± 0.2	155.7 ± 16.2	3.4 ± 0.4
8	3.2 ± 0.1	1414 ± 98	126.6 ± 22.4	50.3 ± 9.0	8.6 ± 1.5	35.7 ± 8.7	6.2 ± 1.5	79.7 ± 0.1	128.8 ± 23.0	3.0 ± 0.5
9	3.4 ± 0.2	1326 ± 34	90.4 ± 1.5	31.8 ± 0.5	6.3 ± 0.4	24.0 ± 0.7	4.8 ± 0.4	79.3 ± 0.1	142.5 ± 14.9	3.2 ± 0.4
10	4.0 ± 0.3	1242 ± 84	114.2 ± 12.0	30.0 ± 2.6	4.8 ± 0.1	23.5 ± 2.6	3.8 ± 0.1	79.2 ± 0.5	146.7 ± 15.1	2.3 ± 0.6
11	3.7 ± 0.1	1330 ± 19	95.8 ± 8.1	31.6 ± 5.0	6.2 ± 0.8	23.8 ± 3.5	4.7 ± 0.6	79.9 ± 0.4	162.5 ± 23.1	3.3 ± 0.5
12	3.3 ± 0.1	1350 ± 18	97.0 ± 9.3	37.6 ± 3.3	7.0 ± 0.9	27.8 ± 2.2	5.2 ± 0.6	79.3 ± 0.4	178.6 ± 19.5	4.3 ± 0.7
13	3.5 ± 0.2	1318 ± 47	111.1 ± 11.4	34.9 ± 5.8	6.5 ± 0.7	26.5 ± 4.6	4.9 ± 0.7	79.3 ± 0.1	144.3 ± 16.2	3.1 ± 0.3
14	3.5 ± 0.1	1332 ± 17	109.6 ± 8.7	38.0 ± 3.1	6.5 ± 0.7	28.5 ± 2.5	4.9 ± 0.6	79.4 ± 0.3	150.0 ± 20.7	3.2 ± 0.5

t thickness, *d* density, *F* breaking load for bending, σ_f maximum flexural strength, E_f elastic modulus, σ_f/d maximum specific flexural strength, E_f/d specific elastic modulus, *W* energy absorbed during the Charpy impact test, *K* impact resilience

Table 6 Coefficients of the best-fit second-order response for each of the fiberboard characteristics analyzed, and corresponding correlation coefficient (R^2)

Coefficient	Density	Bending properties					Surface hardness	Impact strength	Water sensitivity		Color	
	d (kg/m^3)	F (N)	σ_f (MPa)	E_f (GPa)	σ_f/d (kPa m^3/kg)	E_f/d (MPa m^3/kg)	Shore *D* (°)	K (kJ/m^2)	TS (%)	WA (%)	L*	ΔE*
a_0	1325.0	110.3	36.4	6.5	28.0	4.910	79.3	3.2	16.7	10.5	68.3	19.7
a_1	-23.9^{S}	-16.7^{S}	-6.9^{S}	-1.1^{S}	-5.0^{S}	-0.749^{S}	-0.5^{S}	-0.3^{S}	-0.6^{NS}	-1.1^{NS}	-0.3^{S}	0.4^{S}
a_2	-41.5^{S}	34.4^{S}	4.6^{S}	0.0002^{NS}	5.0^{S}	0.176^{S}	0.3^{S}	-0.9^{S}	-9.1^{S}	-7.7^{S}	-1.1^{S}	1.9^{S}
a_3	4.5^{NS}	-7.3^{S}	-2.4^{NS}	-0.4^{S}	-1.0^{NS}	-0.261^{S}	-0.1^{NS}	0.5^{S}	-1.1^{NS}	0.2^{NS}	0.7^{S}	-1.1^{S}
a_{11}	-20.0^{NS}	-10.3^{S}	-3.4^{NS}	-1.4^{S}	-2.0^{NS}	-1.039^{S}	-0.3^{NS}	-0.3^{S}	3.1^{S}	3.1^{S}	-0.2^{NS}	0.3^{NS}
a_{22}	3.0^{NS}	-7.5^{S}	0.8^{NS}	0.5^{S}	1.0^{NS}	0.432^{S}	0.2^{NS}	-0.1^{NS}	4.7^{S}	8.5^{S}	1.4^{S}	-2.1^{S}
a_{33}	13.2^{NS}	-4.4^{S}	-0.9^{NS}	-0.1^{S}	-1.0^{NS}	-0.175^{S}	0.0^{NS}	0.2^{NS}	4.7^{S}	3.9^{S}	-0.3^{NS}	0.6^{NS}
a_{12}	121.8^{S}	6.1^{S}	2.7^{NS}	-0.1^{S}	-2.0^{NS}	-0.723^{S}	0.1^{NS}	-1.2^{S}	-10.9^{S}	-12.6^{S}	-1.2^{S}	1.7^{S}
a_{13}	7.1^{NS}	24.1^{S}	10.1^{NS}	0.5^{S}	8.0^{NS}	0.385^{S}	-0.6^{S}	0.3^{NS}	-3.0^{NS}	0.9^{NS}	0.2^{NS}	-0.1^{NS}
a_{23}	82.4^{S}	-1.5^{S}	4.9^{NS}	1.5^{S}	3.0^{NS}	0.963^{S}	0.4^{NS}	0.0^{NS}	5.6^{S}	6.0^{S}	0.8^{S}	-1.1^{S}
R^2	0.84	0.85	0.58	0.52	0.58	0.53	0.82	0.96	0.96	0.94	0.92	0.93

Coefficients with an S in superscript are significant; coefficients with an NS in superscript are non-significant

The binding ability of lignin was demonstrated by a comparison of boards molded from the same extruded fibers and with the same amount of water added at molding. The addition of lignin improved the bending properties of the boards. However, the addition of lignin was less useful if too much water was added at molding. Indeed, a comparison of boards 3 and 6, both of which had a lignin content of 23.3%, showed that the addition of more water at molding (15% for board 3 rather than the 5% for board 6) resulted in a 12% lower maximum flexural strength and elastic modulus. As described above, this was due to the escape of larger amounts of water vapor from the fibrous material when the press opened, resulting in the generation of more defects in board 3. Thus, the fiberboard with the greatest mechanical resistance to bending in this study was board 8, which was produced with the following molding parameters: 5.0% water added at molding, limiting the tendency for degassing. It was also produced from fibers refined with the minimal L/S ratio during extrusion, resulting in a shorter mean length and a greater specific surface area. Furthermore, in addition to being the most mechanically resistant board, this board was also the densest (Table 5). Fiberboard density and bending properties were clearly correlated. Indeed, with the exception of board 6, which had a maximal lignin content (i.e. 23.3%), higher densities were associated with higher maximum flexural strength (Fig. 4) and a higher elastic modulus (Fig. 5). These findings are consistent with those of a previous study on biodegradable fiberboards made from deoiled sunflower cake by hot pressing (Evon et al. 2015). Not all fiberboards were of the same thickness (from 3.1 to 4.0 mm) and, thus, density. The specific maximum flexural strength and specific elastic modulus, defined as the ratio of bending characteristics to board density were, therefore, also calculated (Table 5). The maximal specific values for both maximum flexural strength and elastic modulus were obtained for board 6, and not for board 8 (Table 5). This fiberboard was produced with the following molding parameters: 5.0% water added at molding (i.e. $X_1 = -0.500$), 23.3% lignin content (i.e. $X_2 = 0.866$), and an L/S ratio of 0.7 during extrusion (i.e. $X_3 = 0.000$). The results for specific bending properties confirmed that the addition of lignin improves the mechanical properties of the fiberboard, as demonstrated by comparisons of boards 5 and 3, or boards 4 and 6. By contrast, the addition of too much water at molding did not improve the final properties of the boards, due to the occurrence of degassing phenomena, thus cracks in the boards. However, the addition of a small amount of water (5%) was required to improve lignin mobilization and plasticization (Orliac et al. 2003; Xu et al.

2006; Yamashita et al. 2009; Takahashi et al. 2010; Pintiaux et al. 2015). Finally, these findings also demonstrate that a low (0.4) or medium (0.7) L/S ratio during extrusion, leading to a shortening of fibers in the extrudate and, thus, to a decrease in aspect ratio, from 15.0 for an L/S ratio of 1.0 to 11.3 for an L/S ratio of 0.4 (Table 4), provides better resistance of the board to bending. The most likely reasons for this include (1) the facilitation of compaction on thermopressing associated with these shorter fibers, (2) their greater specific surface area, and (3) easier access to the cell wall components of rice straw (Shen 1986).

The isoresponse curves for maximum flexural strength and maximum specific flexural strength are shown in Fig. 6. The curves for elastic modulus and specific elastic modulus are represented in Fig. 7. These isoresponse curves illustrate the influence of the molding parameters on the bending properties of the boards. At an L/S ratio of 0.7 for extrudate production (i.e. $X_3 = 0.0$), both maximum flexural strength and maximum specific flexural strength tended to increase with increasing lignin content and decreasing amounts of water added at molding (Fig. 6a, d). At a lignin content of 12.5% (i.e. $X_2 = 0.0$) with the addition of large amounts of water, both maximum flexural strength and maximum specific flexural strength tended to increase with increasing L/S ratio during extrusion (Fig. 6b, e). By contrast, for the addition of small amounts of water, these isoresponse curves also revealed that bending strength increased with decreasing L/S ratio for extrudate production. However, a comparison of these two opposite effects revealed a greater increase in bending strength for the addition of small amounts of water and the use of a low L/S ratio for extrusion than for the addition of large amounts of water and a high L/S ratio.

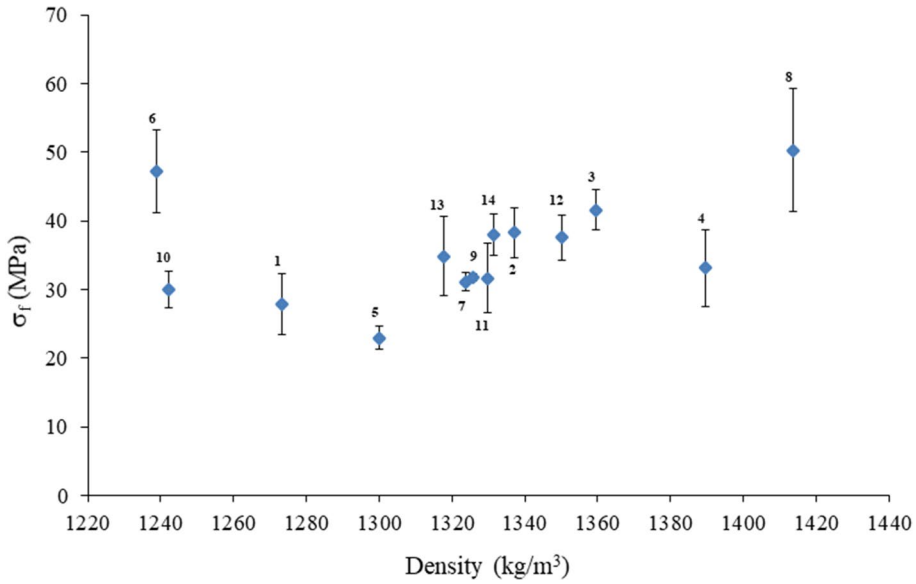

Fig. 4 Maximum flexural strength of fiberboards as a function of their density (the numbers in the figure are the board numbers)

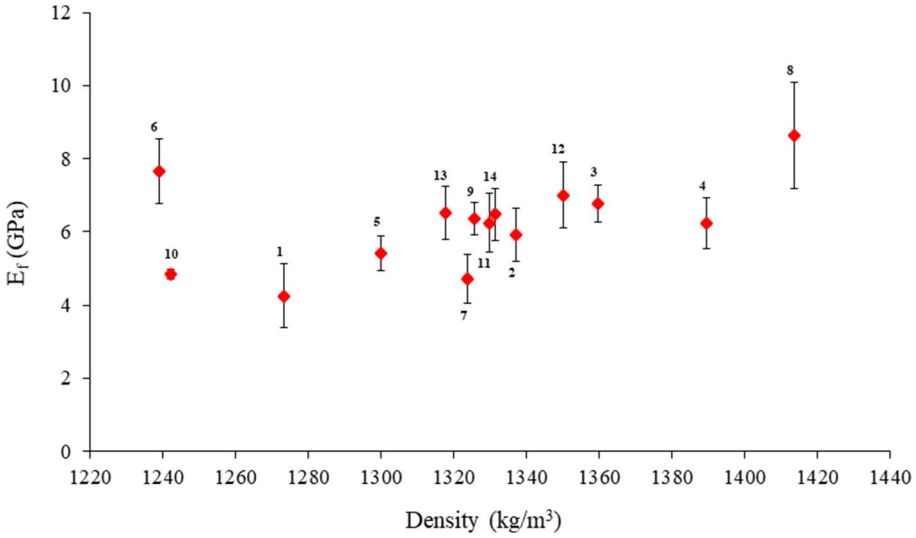

Fig. 5 Elastic modulus of fiberboards as a function of their density (the numbers in the figure are the board numbers)

Finally, Fig. 6c, f show the changes in maximum flexural strength and maximum specific flexural strength as a function of lignin content and the L/S ratio used at extrusion for the addition of 10% water at molding (i.e. $X_1 = 0.0$): the simultaneous addition of more lignin and a gradual lowering of L/S ratio tended to increase the bending strengths of boards. The changes in elastic modulus at an L/S ratio of 0.7 during extrudate production (i.e. $X_3 = 0.0$) are presented in Fig. 7a, d. This modulus increased with decreasing proportions of added water, with an optimal value reached for the addition of about 5% water. Given its binding ability, the addition of larger amounts of lignin with 5% water resulted in a higher specific elastic modulus (Fig. 7d). At a lignin content of 12.5% (i.e. $X_2 = 0.0$), the addition of smaller amounts of water at molding resulted in a more rigid panel, with optimal values for both elastic moduli being obtained for the addition of about 5% water at molding (Fig. 7b, e). In addition, with this optimized level of water addition, boards became increasingly rigid with decreasing L/S ratio at extrusion. Finally, for the addition of 10% water at molding (i.e. $X_1 = 0.0$), the isoresponse curves (Fig. 7c, f) showed an improvement in both elastic and specific elastic moduli when (1) more lignin was added simultaneously with an increase in the L/S ratio used for extrusion, or when (2) lignin content and L/S ratio at extrusion were simultaneously decreased.

Conversely, Shore *D* surface hardness and Charpy impact strength were relatively independent of molding parameters (Table 6). Shore *D* was quite high, with a mean value of 79.3° over the entire Doehlert experiment, due to the high density obtained for all fiberboards manufactured. By contrast, boards were not highly resistant to impact, with a mean impact resilience of only 3.2 kJ/m^2 (Table 6). This fragility

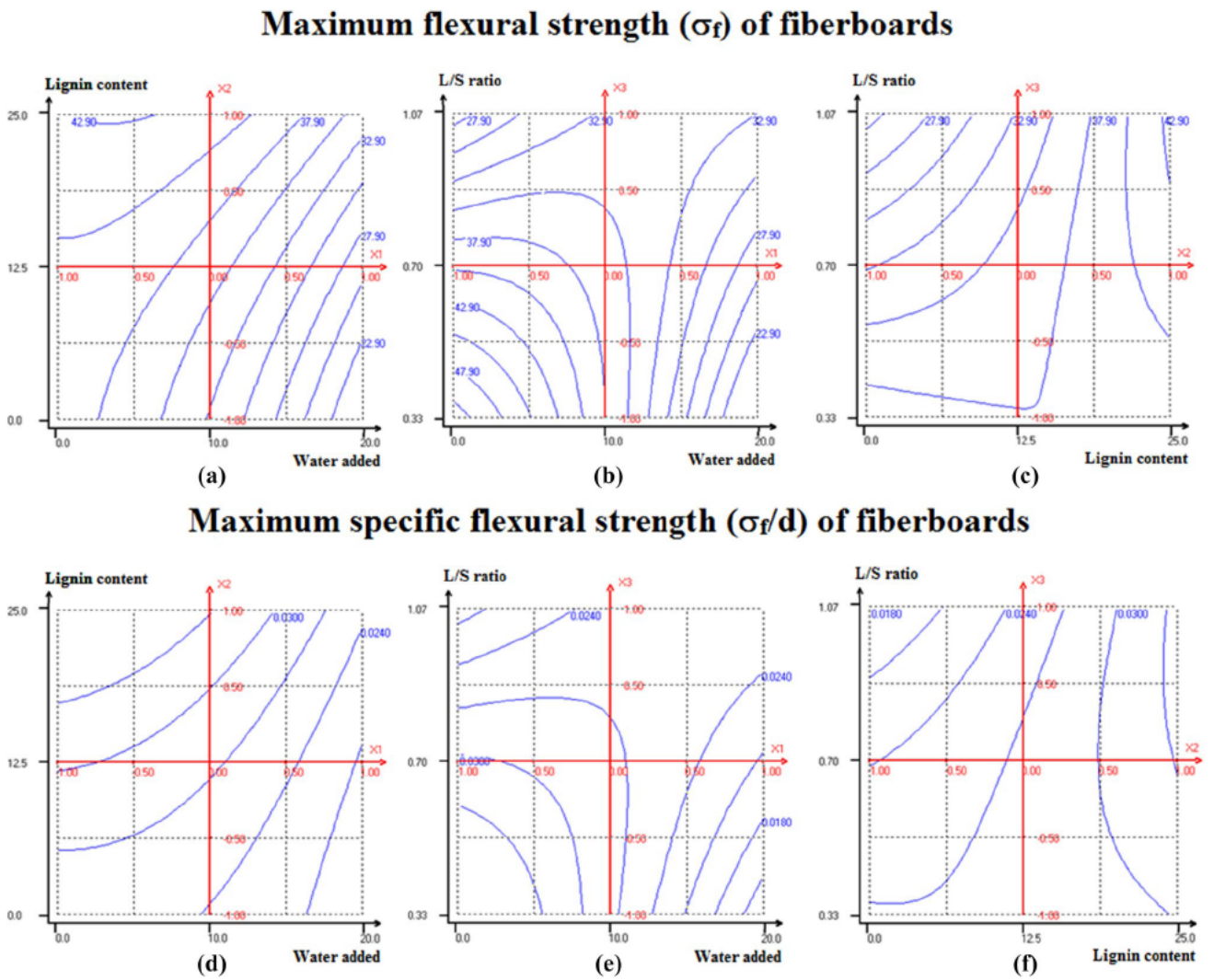

Fig. 6 Isoresponse curves for the maximum flexural strength (σ_f) of fiberboards **a** at an L/S ratio of 0.7 for extrudate production, **b** at a lignin content of 12.5%, and **c** with the addition of 10% water at molding, and curves for maximum specific flexural strength (σ_f/d) **d** at an L/S ratio of 0.7 for extrudate production, **e** at a lignin content of 12.5%, and **f** with the addition of 10% water at molding

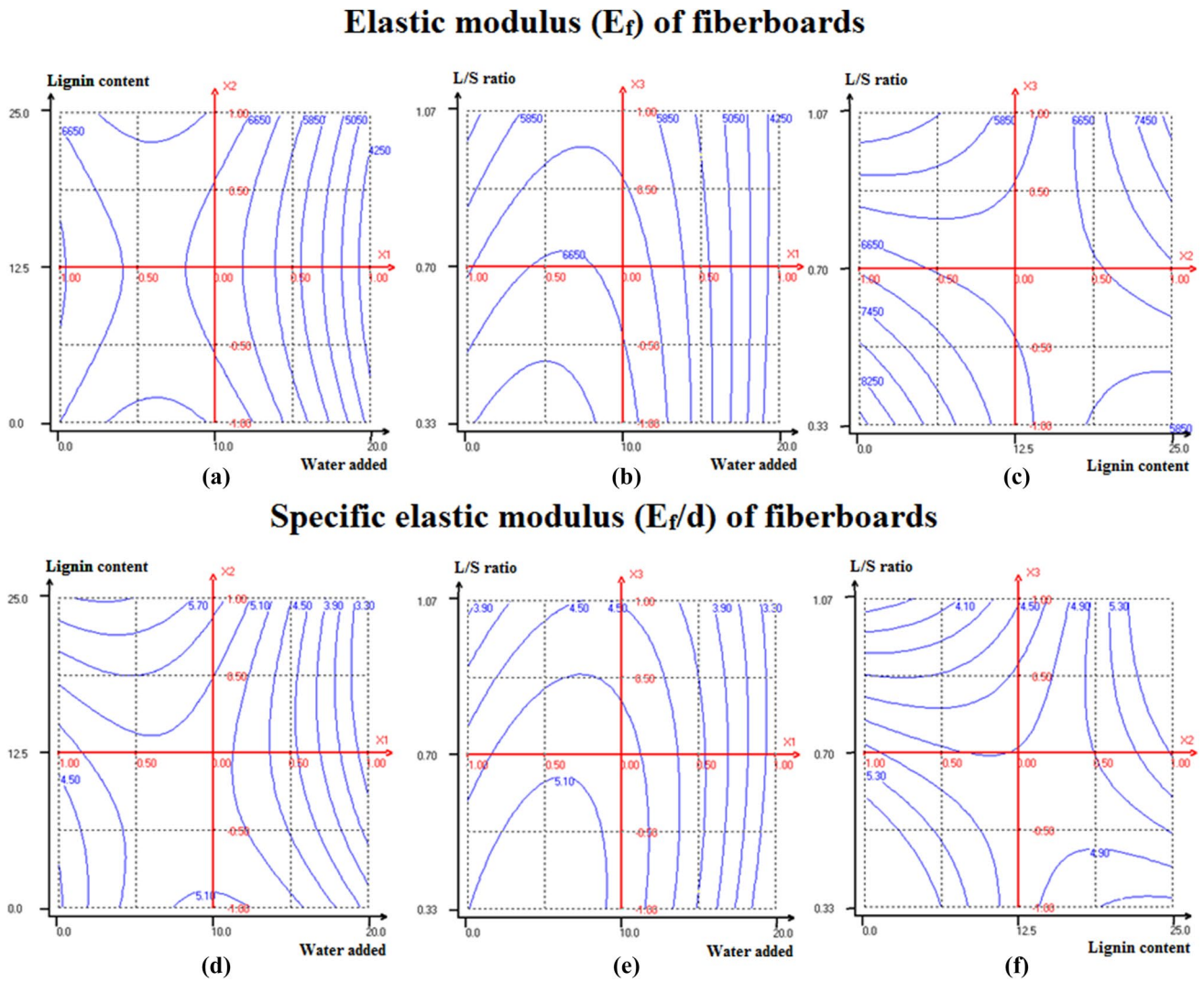

Fig. 7 Isoresponse curves for the elastic modulus (E_f) of fiberboards **a** at an L/S ratio of 0.7 for extrudate production, **b** at a lignin content of 12.5%, and **c** with the addition of 10% water at molding, and curves for specific elastic modulus (E_f/d) **d** at an L/S ratio of 0.7 for extrudate production, **e** at a lignin content of 12.5%, and **f** with the addition of 10% water at molding

was probably due to the high level of rigidity of the boards produced (Table 5). These results are consistent with those of a previous study by Evon et al. (2015) on boards generated from whole sunflower plants.

The thickness swelling (TS) and water absorption (WA) of fiberboards were both influenced by the molding parameters (Table 6). The negative values of a_1 and, particularly, a_2 coefficients in the associated polynomial models clearly indicated that the addition of more water at molding and higher lignin contents in particular were associated with greater water resistance in the fiberboards produced. The maximal TS and WA values were 35% and 32%, respectively, both for panel 5 (Table 7). The lowest values were only 10% and 7%, respectively, both for panel 3 (15% water added, lignin content of 23.3% and an L/S ratio of 0.7 at extrusion). The isoresponse curves for thickness swelling are presented in Fig. 8. In particular, at an L/S ratio of 0.7 at extrusion (i.e. $X_3 = 0.0$), thickness swelling decreased rapidly (i.e. from a maximum value of 35% to less than 10%) with simultaneous increases in both the amount of water added at molding and lignin content (Fig. 8a). Thus, the boards least sensitive to water (TS values of 10–12%) were obtained in the molding conditions with the highest levels of lignin (Fig. 8a, c) together with L/S ratios below 0.7 (Fig. 8c).

Polynomial models were used to determine the optimal responses for each fiberboard characteristic analyzed: density, bending properties, impact resilience, Shore *D* surface hardness, and thickness swelling. All optimal responses and the relevant molding conditions are shown in Table 8. The optimal molding variables were not identical for all characteristics studied. The optimal X_1 coding value was −1.0 (i.e. 0% water added) for density, breaking load, maximum

flexural strength, maximum specific flexural strength, and shore *D* surface hardness. The other optimal X_1 coding values were about −0.55 (i.e. 4.5% water added) for modulus of elasticity and specific modulus of elasticity, and 1.0 (i.e. 20% water added) for Charpy impact strength and thickness swelling. The optimal X_2 coding value was mostly 1.0 (i.e. 25% lignin content), particularly for breaking load, maximum specific flexural strength, specific elastic modulus, Shore *D* surface hardness, and thickness swelling (Table 8). Finally, the optimal X_3 coding value was −1.0 (i.e. an L/S ratio of 0.33 at extrusion) for board density and bending properties. By contrast, it was 1.0 for surface hardness and Charpy impact strength, and −0.16 for thickness swelling.

An additional analysis was also performed to identify the most appropriate parameters to ensure that all the characteristics studied were as close as possible to the optimal values identified in this study (Table 8). The corresponding X_1, X_2, and X_3 coding values were −1.0, 1.0 and −1.0, respectively, corresponding to the following molding parameters: 0% water added at molding, addition of 25% lignin, and an L/S ratio of 0.33 for extrudate production (Table 9). Based on these parameters and the polynomial models for each fiberboard characteristic analyzed, the optimized thermopressed material should have a density of 1102 kg/m^3 rather than the maximal density of 1593 kg/m^3 (i.e. 31% reduction). The maximum flexural strength and the elastic modulus would be approximately 50 MPa and 6.0 GPa, respectively.

Table 7 Physical properties of the 14 fiberboards manufactured by thermopressing

Board number	TS (%)	WA (%)	Color measurements			
			L*	a*	b*	ΔE*
1	17.3±3.5	11.3±1.2	67.5±0.6	1.5±0.5	2.5±0.7	20.7
2	22.3±1.7	15.8±4.4	68.7±1.5	1.5±0.6	3.5±1.6	19.1
3	10.1±2.5	6.6±1.0	67.8±0.7	1.2±0.3	2.5±0.7	20.5
4	22.4±2.2	17.8±1.3	69.7±1.2	2.6±0.5	5.1±1.3	17.3
5	35.2±7.6	31.8±9.0	71.1±1.8	3.0±0.5	6.5±1.7	15.2
6	16.2±3.2	14.3±3.6	68.4±1.3	1.3±0.5	3.1±1.2	19.7
7	15.6±4.2	11.5±1.9	68.4±0.9	1.5±0.7	3.1±1.3	19.6
8	23.6±2.7	17.6±2.7	68.0±0.7	1.4±0.6	2.8±0.9	20.1
9	28.4±2.8	17.5±3.9	67.8±0.6	1.3±0.5	2.6±0.8	20.5
10	14.3±1.4	9.5±0.7	67.2±0.4	0.9±0.2	1.8±0.5	21.4
11	21.8±0.9	17.4±5.1	69.0±1.0	1.7±0.6	4.0±1.3	18.6
12	23.3±1.4	16.7±4.1	69.1±1.7	1.9±0.8	4.1±1.9	18.3
13	16.5±1.9	10.9±0.6	68.4±1.1	1.6±0.6	3.3±1.3	19.5
14	16.9±1.9	12.1±1.3	68.1±1.0	1.5±0.7	3.1±1.3	19.9

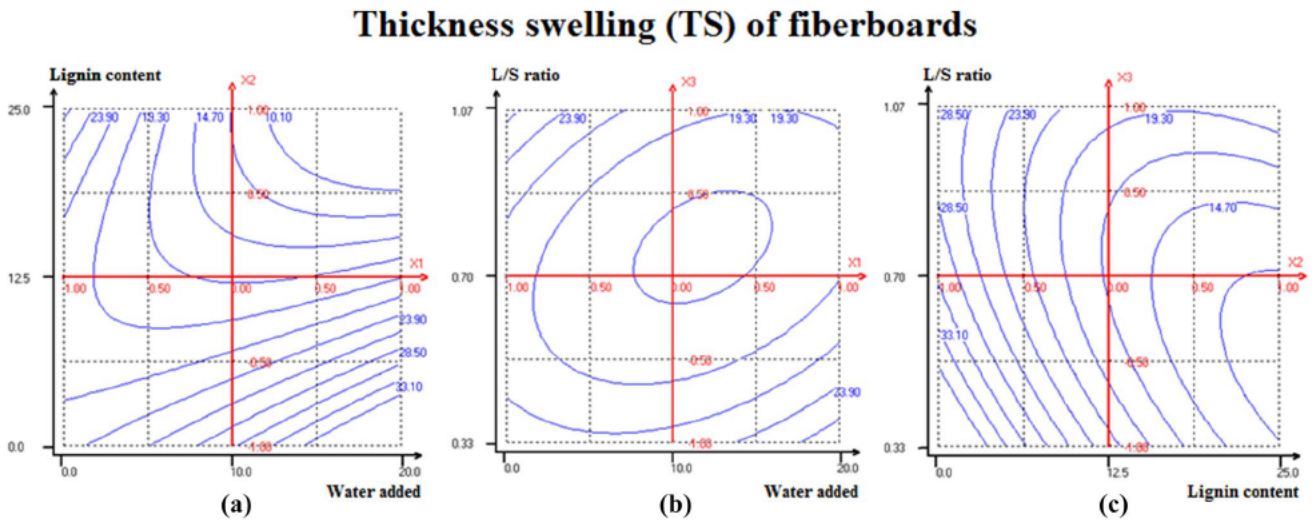

Fig. 8 Isoresponse curves for the thickness swelling (TS) of fiberboards **a** at an L/S ratio of 0.7 for extrudate production, **b** at a lignin content of 12.5%, and **c** with the addition of 10% water at molding

These flexural properties are below the maximal values (i.e. 55 MPa and 9.2 GPa, respectively) but not greatly so, particularly for maximum flexural strength. They are also very similar to the results obtained in other studies of fiberboard production by hot pressing (Anglès et al. 2001; Okuda et al. 2006; Halvarsson et al. 2008, 2009; Mancera et al. 2012; Theng et al. 2015, 2017b).

The bending properties of the optimized board would comply largely with French standard NF EN 312 (a standard dedicated to the specifications for particleboards) for P7-type boards, which are defined as load-bearing boards for use under high stress and in wet conditions (recommendations of 20 MPa and 3 GPa for maximum flexural strength and elastic modulus, respectively, for boards with a thickness of between 3 and 4 mm). Nevertheless, the required thickness swelling of 10% has yet to be achieved. However, an additional process previously demonstrated to be effective (Widyorini et al. 2005; Okuda et al. 2006; Halvarsson et al. 2009; Saadaoui et al. 2013; Evon et al. 2015; Uitterhaegen et al. 2017), such as preheating, chemical treatment, or steam treatment, would probably improve this dimensional stability parameter.

Finally, the optimized board would also have better mechanical resistance than a commercial fiberboard made with eucalyptus and pine wood sawdust as the reinforcing fibers and urea–formaldehyde resin as the binder (42 MPa and 2.7 GPa for maximum flexural strength and elastic modulus, respectively, for this commercial board of similar thickness, i.e. about 3 mm). However, it would be a little denser than this commercial material (i.e. density of 1102 kg/m^3 rather than 883 kg/m^3) (Theng et al. 2015, 2017b).

Table 9 Predicted values calculated from the corresponding polynomial model for each of the fiberboard mechanical properties analyzed for the molding conditions considered to yield a good compromise between density and flexural properties, i.e. 0% water added at molding ($X_1 = -1.00$), 25% lignin content ($X_2 = 1.00$), and an L/S ratio of 0.33 for extrudate production ($X_3 = -1.00$)

Characteristic	Predicted value	Deviation from the optimal value (%)
d (kg/m^3)	1102.0	69.2
F (N)	166.0	100.0
σ_f (MPa)	49.6	89.7
E_f (GPa)	6.0	65.7
σ_f/d (kPa.m^3/kg)	44.0	100.0
E_f/d (MPa.m^3/kg)	5.2	79.6
Shore *D* (°)	79.1	97.9
K (kJ/m^2)	3.5	61.4

In conclusion, the optimized experimental laboratory fiberboard made from rice straw thermomechanical extrudate plus Biolignin™ as a natural binder appeared to provide a good compromise between bending properties and density, resulting in reasonably high mechanical resistance at low density. However, this density was nevertheless slightly higher than that of most commercial hardboards (around 1000 kg/m^3), which could cause some handling difficulties. This higher panel density results from the absence of synthetic resin, the use of thermopressing at high temperature and pressure being necessary to mobilize the lignin-based binder during hot pressing (Tajuddin et al. 2016). The next step in this work will be the optimization of molding conditions, by decreasing the pressure applied and the molding

Table 8 Optimal molding conditions for each of the fiberboard characteristics analyzed, and corresponding optimal response ($Y_{optimal}$)

Characteristic	X_1	Water added at molding (%)	X_2	Lignin content (%)	X_3	L/S ratio during extrusion	$Y_{optimal}$[a]
Bending properties							
d (kg/m^3)	−1.00	0.0	−1.00	0.0	−1.00	0.33	1593.4
F (N)	−1.00	0.0	1.00	25.0	−1.00	0.33	166.0
σ_f (MPa)	−1.00	0.0	−1.00	0.0	−1.00	0.33	55.2
E_f (GPa)	−0.55	4.5	−1.00	0.0	−1.00	0.33	9.2
σ_f/d (kPa.m^3/kg)	−1.00	0.0	1.00	25.0	−1.00	0.33	44.0
E_f/d (MPa.m^3/kg)	−0.52	4.8	1.00	25.00	1.00	1.07	6.56
Surface hardness							
Shore *D* (°)	−1.00	0.0	1.00	25.0	1.00	1.07	80.9
Charpy impact strength							
K (kJ/m^2)	1.00	20.0	−1.00	0.0	1.00	1.07	5.8
Water sensitivity							
TS (%)	1.00	20.0	1.00	25.0	−0.16	0.64	3.7

[a]The optimal response is the maximal response for fiberboard mechanical properties (i.e. flexural properties, Charpy impact strength, and Shore *D* surface hardness), and the minimal response in terms of thickness swelling

time, in particular, whilst maintaining strong mechanical properties. On the one hand, reducing the pressure should decrease board density, making the board easier to handle. On the other, a decrease in molding time would be more economical. This time should be no longer than 30 s per mm thickness to ensure competitiveness in terms of molding costs with commercial particleboards, particularly those produced industrially for indoor use. This molding time corresponds to a maximum of 120 s for a 4 mm-thick fiberboard.

4 Conclusion

Novel biodegradable and cohesive fiberboards were manufactured with a heated hydraulic press from rice straw extrudates produced by thermomechanical pretreatment in a twin-screw extruder, in the absence of a chemical reaction. The lignin and water added at the molding stage served as a natural binder and a lignin plasticizer, respectively, and lignocellulosic fibers also provided mechanical strength. The molding parameters (i.e. the amount of water added at molding, lignin content, and the L/S ratio used for the extrudate production in the twin-screw extruder) influenced the mechanical and physical properties of the boards. The best flexural properties obtained in this Doehlert experimental design corresponded to a board made from the extrudate produced at the lowest L/S ratio for twin-screw extrusion (i.e. 0.4), molded with the addition of 5% water and a lignin content of 8.9%. This material had a high density (i.e. 1414 kg/m^3), and could thus be considered a hardboard; its maximum flexural strength and elastic modulus were 50.3 MPa and 8.6 GPa, respectively. These values were the highest obtained in this study. Thickness swelling and water absorption were 24% and 18%, respectively. This board would largely comply with standard NF EN 312, type P7 (i.e. load-bearing boards for use under high stress and in wet conditions) in terms of bending properties, although post-treatment would be required to improve water resistance (threshold of 10% for thickness swelling). A good compromise between flexural properties and density could be obtained with the following molding parameters: 0% water added at molding, 25% lignin content, and an L/S ratio of 0.33 for extrudate production. The fiberboard produced with such parameters, with no chemical reagent or synthetic resin addition, would have a density of 1102 kg/m^3, a maximum flexural strength of 50 MPa, and an elastic modulus of 6.0 GPa. These properties would comply with French standard NF EN 312, type P7.

Acknowledgements The authors wish to thank the Erasmus + KA107 project for financial support. Special sincere gratitude is given to Laboratoire de Chimie Agro-Industrielle (LCA), INP-ENSIACET, Toulouse, France for providing both raw materials and experimental support, and CIMV for supplying Biolignin™.

References

Anglès MN, Ferrando F, Farriol X, Salvadó J (2001) Suitability of steam exploded residual softwood for the production of binderless panels. Effect of the pre-treatment severity and lignin addition. Biomass Bioenerg 21:211–224

Back EL (1987) The bonding mechanism in hardboard manufacture review report. Holzforsch Int J Biol Chem Phys Technol Wood 41:247–258

CIMV TBC (2014) MSDS (CE) no 453/2010 biolignin. CIMV, France

Domínguez-Robles J, Tarrés Q, Delgado-Aguilar M, Rodríguez A, Espinach FX, Mutjé P (2017) Approaching a new generation of fiberboards taking advantage of self lignin as green adhesive. Int J Biol Macromol 108:927–935

Evon P, Vandenbossche V, Pontalier P-Y, Rigal L (2010) The twin-screw extrusion technology, an original and powerful solution for the biorefinery of sunflower whole plant. In: 18th European biomass conference and exhibition, Lyon, France, Open Archieve Toulouse Archieve Ouverte (OATAO)

Evon P, Vandenbossche V, Pontalier P-Y, Rigal L (2014) New thermal insulation fiberboards from cake generated during biorefinery of sunflower whole plant in a twin-screw extruder. Ind Crops Prod 52:354–362

Evon P, Vinet J, Labonne L, Rigal L (2015) Influence of thermo-pressing conditions on the mechanical properties of biodegradable fiberboards made from a deoiled sunflower cake. Ind Crops Prod 65:117–126

Evon P, Barthod-Malat B, Grégoire M, Vaca-Medina G, Labonne L, Ballas S, Véronèse T, Ouagne P (2018) Production of fiberboards from shives collected after continuous fiber mechanical extraction from oleaginous flax. J Nat Fibers. https://doi.org/10.1080/15440478.2017.1423264

Gosselink RJ, van Dam JE, de Jong E, Gellerstedt G, Scott EL, Sanders JP (2011) Effect of periodate on lignin for wood adhesive application. Holzforsch 65:155–162

Halvarsson S, Edlund H, Norgren M (2008) Properties of medium-density fibreboard (MDF) based on wheat straw and melamine modified urea formaldehyde (UMF) resin. Ind Crops Prod 28:37–46

Halvarsson S, Edlund H, Norgren M (2009) Manufacture of high-performance rice-straw fiberboards. Ind Eng Chem Res 49:1428–1435

Konica Minolta Sensing (2007) Let's study color. In: Precise color communication, Part I. Konica Minolta, Inc., Tokyo

Lin Z, Liu L, Li R, Shi J (2012) Screw extrusion pretreatments to enhance the hydrolysis of lignocellulosic biomass. J Microb Biochem Technol S 12:002. https://doi.org/10.4172/1948-5948.S12-002

Mancera C, El Mansouri N-E, Pelach MA, Francesc F, Salvadó J (2012) Feasibility of incorporating treated lignins in fiberboards made from agricultural waste. Waste Manag 32:1962–1967

Mason W (1928) Process of making structural insulating boards of exploded lignocellulose fiber. MF Company, Laurel

Miki T, Takakura N, Iizuka T, Yamaguchi K, Kanayama K (2003) Possibility of extrusion of wood powders. JSME Int J Ser A Solid Mech Mater Eng 46:371–377

Mobarak F, Fahmy Y, Augustin H (1982) Binderless lignocellulose composite from bagasse and mechanism of self-bonding. Holzforsch Int J Biol Chem Phys Technol Wood 36:131–136

Murugan P, Mahinpey N, Johnson KE, Wilson M (2008) Kinetics of the pyrolysis of lignin using thermogravimetric and differential scanning calorimetry methods. Energ Fuels 22:2720–2724

NEMRODW (2015) A performing software for the design and analysis of experimental plans. http://www.nemrodw.com/idex.php. Accessed 1 Sep 2016

Okuda N, Hori K, Sato M (2006) Chemical changes of kenaf core binderless boards during hot pressing (II): effects on the binderless board properties. J Wood Sci 52:249–254

Orliac O, Rouilly A, Silvestre F, Rigal L (2003) Effects of various plasticizers on the mechanical properties, water resistance and aging of thermo-moulded films made from sunflower proteins. Ind Crops Prod 18:91–100

Ouagne P, Barthod-Malat B, Evon Ph, Labonne L, Placet V (2017) Fibre extraction from oleaginous flax for technical textile applications: influence of pre-processing parameters on fibre extraction yield, size distribution and mechanical properties. Procedia Eng 200:213–220

Pintiaux T, Viet D, Vandenbossche V, Rigal L, Rouilly A (2015) Binderless materials obtained by thermo-compressive processing of lignocellulosic fibers: a comprehensive review. BioResource 10:1915–1963

Saadaoui N, Rouilly A, Fares K, Rigal L (2013) Characterization of date palm lignocellulosic by-products and self-bonded composite materials obtained thereof. Mater Des 50:302–308

Shen KC (1986) Process for manufacturing composite products from lignocellulosic materials. US4627951A Patent

Tajuddin M, Ahmad Z, Ismail H (2016) A review of natural fibers and processing operations for the production of binderless boards. BioResource 11:5600–5617

Takahashi I, Sugimoto T, Takasu Y, Yamasaki M, Sasaki Y, Kikata Y (2010) Preparation of thermoplastic molding from steamed Japanese beech flour. Holzforsch Int J Biol Chem Phys Technol Wood 64:229–234

Theng D (2017) Feasibility of incorporating treated lignin and cellulose nanofiber in fiberboards made from corn stalk and rice straw. Ph.D thesis, University of Girona, Spain

Theng D, Arbat G, Delgado-Aguilar M, Vilaseca F, Ngo B, Mutjé P (2015) All-lignocellulosic fiberboard from corn biomass and cellulose nanofibers. Ind Crops Prod 76:166–173

Theng D, Arbat G, Delgado-Aguilar M, Ngo B, Labonne L, Evon P, Mutjé P (2017a) Comparison between two different pretreatment technologies of rice straw fibers prior to fiberboard manufacturing: twin-screw extrusion and digestion plus defibration. Ind Crops Prod 107:184–197

Theng D, El Mansouri N, Arbat G, Ngo B, Delgado-Aguilar M, Àngels Pelach M, Fullana-i-Palmer P, Mutje P (2017b) Fiberboards made from corn stalk thermomechanical pulp and kraft lignin as green adhesive. BioResource 12:2379–2393

Uitterhaegen E, Nguyen QH, Merah O, Stevens CV, Talou T, Rigal L, Evon P (2016) New renewable and biodegradable fiberboards from a coriander press cake. J Renew Mater 4:225–238

Uitterhaegen E, Labonne L, Merah O, Talou T, Ballas S, Véronèse T, Evon P (2017) Optimization of thermopressing conditions for the production of binderless boards from a coriander twin-screw extrusion cake. J Appl Polym Sci. https://doi.org/10.1002/app.44650

Van Soest PJ, Wine RH (1967) Use of detergents in the analysis of fibrious feeds. IV. Determination of plant cell wall constituents. J Assoc Off Anal Chem 50:50–55

Van Soest PJ, Wine RH (1968) Determination of lignin and cellulose in acid detergent fiber with permanganate. J Assoc Off Anal Chem 51:780–784

Van Dam JE, van den Oever MJ, Teunissen W, Keijsers ER, Peralta AG (2004) Process for production of high density/high performance binderless boards from whole coconut husk: Part 1: lignin as intrinsic thermosetting binder resin. Ind Crops Prod 19:207–216

Vandenbossche V, Brault J, Vilarem G, Rigal L (2015) Bio-catalytic action of twin-screw extruder enzymatic hydrolysis on the deconstruction of annual plant material: case of sweet corn co-products. Ind Crops Prod 67:239–248

Vandenbossche V, Brault J, Hernandez-Melendez O, Evon P, Barzana E, Vilarem G, Rigal L (2016) Suitability assessment of a continuous process combining thermo-mechano-chemical and bio-catalytic action in a single pilot-scale twin-screw extruder for six different biomass sources. Bioresour Technol 211:146–153

Widyorini R, Xu J, Umemura K, Kawai S (2005) Manufacture and properties of binderless particleboard from bagasse I: effects of raw material type, storage methods, and manufacturing process. J Wood Sci 51:648

Xu J, Widyorini R, Yamauchi H, Kawai S (2006) Development of binderless fiberboard from kenaf core. J Wood Sci 52:236

Yamashita O, Imanishi H, Kanayama K (2007) Transfer molding of bamboo. J Mater Process Technol 192:259–264

Yamashita O, Yokochi H, Miki T, Kanayama K (2009) The pliability of wood and its application to molding. J Mater Process Technol 209:5239–5244

Zhang D, Zhang A, Xue L (2015) A review of preparation of binderless fiberboards and its self-bonding mechanism. Wood Sci Technol 49:661–679